

Exploring Dark Knowledge under Various Teacher Capacities and Addressing Capacity Mismatch

Xin-Chun Li*, Wen-Shu Fan*, Bowen Tao, Le Gan, and De-Chuan Zhan

Abstract—Knowledge Distillation (KD) could transfer the “dark knowledge” of a well-performed yet large neural network to a weaker but lightweight one. From the view of output logits and softened probabilities, this paper goes deeper into the dark knowledge provided by teachers with different capacities. Two fundamental observations are: (1) a larger teacher tends to produce probability vectors that are less distinct between non-ground-truth classes; (2) teachers with different capacities are basically consistent in their cognition of relative class affinity. Abundant experimental studies verify these observations and in-depth empirical explanations are provided. The difference in dark knowledge leads to the peculiar phenomenon named “capacity mismatch” that a more accurate teacher does not necessarily perform as well as a smaller teacher when teaching the same student network. Enlarging the distinctness between non-ground-truth class probabilities for larger teachers could address the capacity mismatch problem. This paper explores multiple simple yet effective ways to achieve this goal and verify their success by comparing them with popular KD methods that solve the capacity mismatch.

Index Terms—Knowledge distillation, dark knowledge, capacity mismatch, non-ground-truth class, temperature scaling

I. INTRODUCTION

DEPLOYING large-scale neural networks on portable devices with limited computation and storage resources is challenging [1], and efficient architectures such as MobileNets [2], [3] and ShuffleNets [4], [5] have been designed for lightweight deployment. However, the performances of these lightweight networks are usually not comparable to the larger ones. Commonly, second learning [6], [7] or knowledge distillation (KD) [8]–[10] could be utilized to transfer the knowledge of a more complex and well-performed network (i.e., the teacher) to the smaller ones (i.e., the student). The dark knowledge in KD is still a mystery that has attracted lots of studies [9], [11]–[13], and their goal is to answer the following question: what’s the knowledge that the teacher provides and why they are effective in KD?

In the original KD method [9], the student aims to mimic the teacher’s behavior by minimizing the Kullback-Leibler (KL) divergence between their output probabilities. That is, the logits and softened probabilities, i.e., the inputs to the final softmax operator and the corresponding outputs, are the

specific knowledge transferred in KD. With the development of KD methods, the output-level knowledge has been extended to various types [14], including the intermediate features [15]–[20], the sample relationships [21]–[27], the parameters [28], [29], and the collaborative or online knowledge [10], [30] etc. However, the outputs of neural networks are much easier to visualize, analyze, and understand. Therefore, we focus on the original KD [9] and aim to understand the dark knowledge (i.e., the logits and softened probabilities) provided by the teachers. Unlike previous studies, we majorly study the output-level dark knowledge provided by teachers *with various capacities*, which receives little attention in previous studies. We first present two significant observations: (1) an over-confident teacher tends to produce probability vectors that are less distinct between non-ground-truth classes; (2) teachers with different capacities are basically consistent in their cognition of relative class affinity. The first observation tells the difference between dark knowledge provided by teachers with different capacities, while the second observation shows the consistency between them.

This paper first explains the reasons for the first observation. Larger teachers generally have powerful feature extractors, making the features of the same class more compact and the features between classes more dispersed. Hence, more complex teachers are over-confident and assign a larger score for the ground-truth class or less varied scores for the non-ground-truth classes. If we use a uniform temperature to scale their logits, the probabilities of non-ground-truth classes are less distinct [31], further making the distillation process ineffective. This explains the peculiar phenomenon named “capacity mismatch” [31]–[36] in KD that a more accurate teacher does not necessarily make better students. Fortunately, the second observation ensures that the dark knowledge from teachers with various capacities is basically consistent in the class relative probabilities. We first provide several definite metrics to verify the observation, including the rank of set overlap, Kendall’s τ , and the Spearman correlation. These metrics are irrelevant to the absolute probability values between classes, which are appropriate for measuring the correlation of relative class affinities. We also present the two observations together via the group classes in CIFAR-100 [37] and a constructed group classification task based on Digits-Five [38].

These two observations imply that complex teachers know approximately the same as smaller teachers on relative class affinities, while their absolute probabilities are not discriminative between non-ground-truth classes. Hence, to improve the quality of the dark knowledge provided by complex teachers, an intuitive way is to enlarge the distinctness between non-ground-truth classes. We propose several simple yet effective

Xin-Chun Li, Wen-Shu Fan, Bowen Tao, Le Gan and De-Chuan Zhan are with the School of Artificial Intelligence, National Key Laboratory for Novel Software Technology, Nanjing University, Nanjing, Jiangsu 210023, China. E-mail: lixc@lamda.nju.edu.cn, fanws@lamda.nju.edu.cn, taobw@lamda.nju.edu.cn, ganle@nju.edu.cn, zhandc@nju.edu.cn.

* represents the equal contribution. De-Chuan Zhan is the corresponding author.

This is the extended version of the paper published in the conference of NeurIPS 2022 [31].

methods to enlarge the distinctness of non-ground-truth class probabilities, which could make the distillation process more discriminative. Abundant experimental studies verify that the proposed methods could address the capacity mismatch problem effectively.

We summarize our contributions as two aspects: (1) showing novel insights about the dark knowledge provided by teachers with various capacities, including their distinctness on absolute class probabilities and consistency in relative class affinities; (2) addressing the capacity mismatch problem in KD by proposing multiple simple yet effective methods, which are verified by abundant experimental studies.

II. RELATED WORKS

Our work is closely related to the dark knowledge and capacity mismatch problem in KD.

A. Dark Knowledge in KD

Quite a few works focus on understanding and revealing the essence and effects of “dark knowledge” in KD, including the empirical studies and theoretical analysis [11]–[13], [32], [39]–[44]. [11] unifies the dark knowledge with privileged information, and [45] attributes the dark knowledge in vision tasks to the task-relevant and task-irrelevant visual concepts. The dark knowledge in KD is also related to label smoothing (LS) [41], [46], [47]. Some works decompose the dark knowledge of teachers and aim to understand their effectiveness correspondingly. [48] decomposes the dark knowledge into two parts, explaining the teacher’s ground-truth/non-ground-truth outputs as importance weighting and class similarities. [39] decomposes the dark knowledge into three parts including universal knowledge, domain knowledge, and gradient rescaling. The bias-variance decomposition is also utilized to analyze the property of KD [13], [43]. [49] utilizes the standard deviation of the secondary soft probabilities to reflect the quality of the teachers’ dark knowledge. The most related work [31] decomposes the KD into correct guidance, smooth regularization, and class discriminability, which provides novel insights about the key information in the dark knowledge. Few works have examined the relationship of dark knowledge with teacher capacities, and this paper provides detailed observations and analysis about this.

B. Capacity Mismatch in KD

An intuitive sense after the proposal of KD [9] is that larger teachers could teach students better because their accuracy is higher. However, there exists a peculiar phenomenon named capacity mismatch that excellent teachers can’t completely teach the smaller students well. ESKD [32] first points out the phenomenon and points out that teacher accuracy may poorly predict the student’s performance, i.e., more accurate neural networks don’t necessarily teach better. TAKD [33] solves this problem by introducing an intermediate-sized network (i.e., the teacher assistant) to bridge the knowledge transfer between networks with a large capacity gap. SCKD [34] formulates KD as a multi-task learning problem with several knowledge

transfer losses. ResKD [35], [36] utilize the “residual” of knowledge to teach the residual student, and then take the ensemble of the student and residual student for inference. DIST [50] finds that the discrepancy between the student and a stronger teacher may be fairly severe, which disturbs the training process, and they propose a ranking-based loss as the solution. [51] advocates that an intermediate checkpoint will be more appropriate for distillation. [52] explores the strong teachers in few-shot learning. [53] studies the effect of capacity gap on the generated samples in data-free KD. One of our methods is closely related to [31] that proposes Asymmetric Temperature Scaling (ATS) to make the larger networks teach well again. An improved version named Instance-Specific ATS (ISATS) is proposed. Aside from this method, we also propose other simple yet effective solutions from different aspects.

III. BACKGROUND AND PRELIMINARIES

We follow the basic notations as introduced in [31]. Specifically, we consider a C -class classification problem with $\mathcal{Y} = [C] = \{1, 2, \dots, C\}$. We denote the “logits” as the output scores of a sample \mathbf{x} before applying the softmax function, which is represented as $\mathbf{f}(\mathbf{x}) \in \mathbb{R}^C$. Correspondingly, the softened probability vector is denoted as $\mathbf{p}(\mathbf{x}; \tau) = \text{SF}(\mathbf{f}(\mathbf{x}); \tau)$, where $\text{SF}(\cdot; \tau)$ denotes the softmax function with temperature τ . \mathbf{f}_y and \mathbf{p}_y denote the ground-truth class’s logit and probability, while $\mathbf{g} = [\mathbf{f}_c]_{c \neq y}$ and $\mathbf{q} = [\mathbf{p}_c]_{c \neq y}$ represent the vector of non-ground-truth classes’ logits and probabilities. y denotes the ground-truth class.

The most standard KD [9] contains two stages of training. The first stage trains complex teachers, and then the second stage transfers the knowledge from teachers to a smaller student by minimizing the KL divergence between softened probabilities. Usually, the loss function during the second stage (i.e., the student’s learning objective) is a combination of cross-entropy loss and distillation loss:

$$\ell = -(1 - \lambda) \log \mathbf{p}_y^s(1) - \lambda \tau^2 \sum_{c=1}^C \mathbf{p}_c^t(\tau) \log \mathbf{p}_c^s(\tau), \quad (1)$$

where the upper script “t”/“s” denotes “teacher”/“student” respectively. The dark knowledge in the above distillation equation is the teacher’s label, i.e., $\mathbf{p}^t(\tau)$. In this paper, we aim to study the influence of teacher capacity on the teacher’s label. That is, we majorly compare the relationships between $\mathbf{p}^{t_{\text{large}}}$ and $\mathbf{p}^{t_{\text{small}}}$ which are provided by a larger and a smaller teacher, denoted as t_{large} and t_{small} , respectively.

Commonly, the training and test accuracy of t_{large} will be higher than that of t_{small} because the larger teacher has a huge capacity to capture more information. The process of KD has the effect of improving the student network’s performance when compared with its independent training. An explanation for this improvement is that the dark knowledge contained in larger teachers could help the student better capture the semantic information. Hence, to further improve the performance of the student network, a natural idea is replacing the smaller teacher (i.e., t_{small}) with a larger one (i.e., t_{large}). Frustratingly, this leads to a degradation in the performance of the student network. This phenomenon is named the “capacity

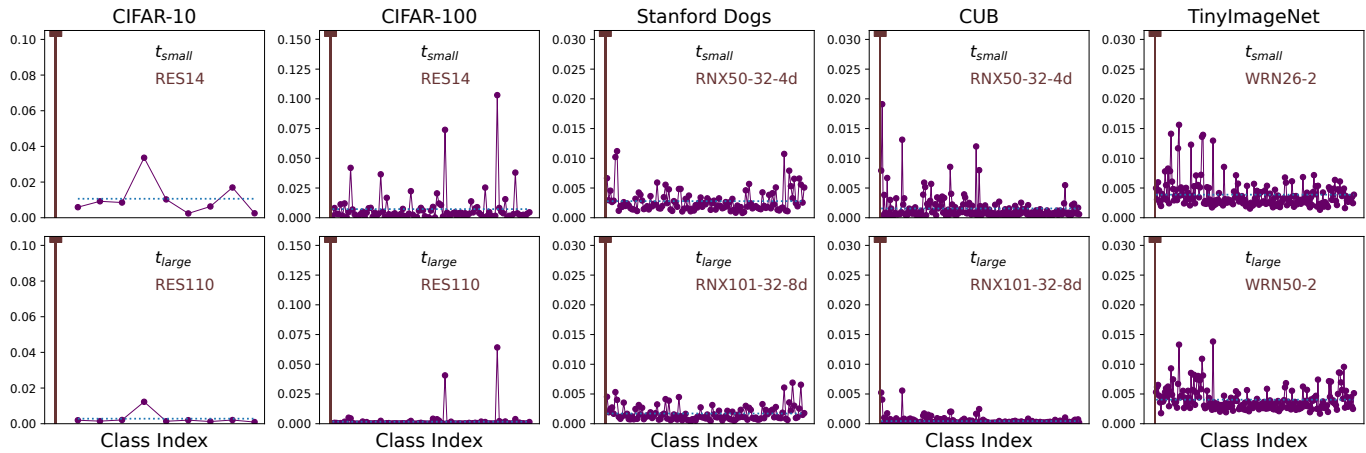


Fig. 1. Visualization of softened probability vectors. The first/second row shows results provided by smaller/larger teachers on the same sample with the same temperature. The first bar shows the ground-truth class while others are non-ground-truth classes. Two observations: (1) the non-ground-truth class probabilities shown in the second row are less varied; (2) the relative class probabilities are nearly the same between the first and second rows.

mismatch” in KD, which is still counter-intuitive, surprising, and unexplored as declared in previous studies [33], [34], [36]. This paper will propose multiple simple yet effective methods to tackle the performance degradation problem.

IV. OBSERVATIONS AND EXPLANATIONS

We first present two observations about the influence of teacher capacities on dark knowledge. Then, we provide explanations and metrics to better understand the findings.

A. Observations

An intuitive method to reflect the relationship of dark knowledge produced by teachers with various capacities is visualization. The first step is training teacher networks with different capacities on several benchmarks. Specifically, this paper trains ResNet14 and ResNet110 [54] on the CIFAR-10/CIFAR-100 dataset [37], and trains ResNeXt50-32-4d and ResNeXt101-32-8d [55] on the Stanford Dogs [56] and CUB [57] dataset, and trains WideResNet26-2 and WideResNet50-2 [58] on the TinyImageNet [59] dataset. Then, for each dataset, a random sample is sampled from the first class in the training set and the softened probability vectors produced by different teachers are visualized. Fig. 1 shows the results, where “RES”, “RNx”, and “WRN” are abbreviations for corresponding networks. The utilized temperature is common across the subfigures. Comparing the first and second rows, it is obvious that larger teachers provide less varied probabilities for non-ground-truth classes. Although the variance of non-ground-truth class probabilities differs a lot between teachers, the relative probability values seem to be consistent. For example, the several highest bars between the two rows lie nearly in the same classes. We conclude the two fundamental observations as follows: (1) *larger teachers tend to produce probability vectors that are less distinct between non-ground-truth classes*; (2) *teachers with different capacities are basically consistent in their cognition of relative class affinity*. To further support these two observations, we provide explanations and statistical measures in the following.

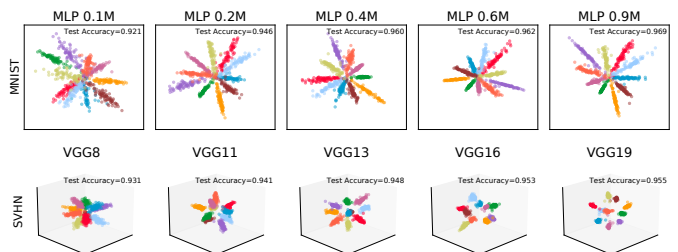


Fig. 2. Visualization of extracted features by teachers with increasing capacities. The first row shows the extracted 2-dim features on MNIST, and the second shows the 3-dim features on SVHN. The accuracy on the test set is also reported.

B. The Variance of Non-ground-truth Class Probabilities

The explanations for the first observation are provided step by step. First, we train MLP networks on MNIST [60] and train VGG [61] networks on SVHN [62]. These two datasets are relatively simpler classification tasks, and we set the final feature dimensions as 2 and 3 correspondingly for better visualization. We do not use the bias parameters in the last layer. We progressively enlarge the depth and width of MLP networks, and use the total number of parameters to denote the network capacity. The capacity of MLP networks ranges from 0.1M to 0.9M. The VGG capacities are determined by the number of layers, which ranges from 8 to 19. We do not use ReLU [63] activation for the final extracted features. These two datasets have 10 types of digits to identify, and the extracted features are scattered in Fig. 2. With the capacity increases, the features of the same class are more compact, while the class centers between different classes are more dispersed. Notably, the larger networks do not overfit the training dataset, because the test accuracy shown in the figure still becomes higher. This implies that larger DNNs obtain a higher performance but may extract more compact intra-class features and more dispersed inter-class features.

The above demos show low-dimensional features that may not reflect the change in high-dimensional space. Hence, we

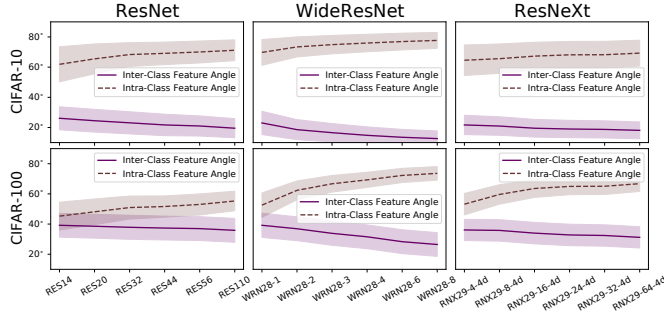


Fig. 3. The change of inter-class and intra-class feature angle under different teacher capacities. The x-axis in each subfigure shows the teacher capacity.

extend the findings to CIFAR-10 and CIFAR-100, on which we train a series of ResNet, WideResNet, and ResNeXt networks. Because the high-dimensional features are hard to visualize and the dimensional-reduced plots by T-SNE [64] are sensitive to hyper-parameters, we instead calculate several metrics to indirectly verify the change of feature compactness. Specifically, we calculate the feature angle as follows:

$$\mathcal{A}(i, j) = \arccos \left(\frac{\mathbf{h}_i^T \mathbf{h}_j}{\|\mathbf{h}_i\| \|\mathbf{h}_j\|} \right), \quad (2)$$

where \mathbf{h}_i and \mathbf{h}_j are feature vectors of the i -th and j -th training sample. Then, we define the inter-class and intra-class set as $\{(i, j)\}_{y_i=y_j, \forall i, j}$ and $\{(i, j)\}_{y_i \neq y_j, \forall i, j}$, respectively. The average and standard deviation of angles in the two sets are plotted in Fig. 3. If the teacher becomes more complex, the inter-class feature angle becomes smaller, while the intra-class angle becomes larger. Notably, we use ReLU [63] activation before the classification layer, implying that all of the elements in the extracted features are non-negative. This could already provide some hints for the capacity mismatch phenomenon. As an extreme case, if the features among the same class collapse into a single point, and features among different classes are orthogonal to each other, the inter-class feature angle will be zero and the intra-class one will be 90° . Although the training and test accuracy will be 100%, the softened probabilities may be one-hot labels, which bring no additional information to the student. An illustration and more detailed discussion can be found in Sect. VII. The inter-class and intra-class distance metrics utilized in linear discriminant analysis [65] or unsupervised discriminant projection [66] show the same trend. We omit the display of the results based on these distance metrics because the trends of feature angles are vivid enough to show how the feature compactness changes.

According to the softmax properties in classification problems, the classification weight of each class is pulled towards the features from the same class while pushed away from the features of other classes [67]. That is, the change tendency of features could partially reflect the tendency of classification weights in the final layer. An ideal case is that the learned classification weights converge to the feature centers. If the intra-class feature angle becomes larger, the feature of a specific sample will be far away from the classification weights of the other classes. Similarly, the feature of a specific sample will be closer to the corresponding class's classification weight.

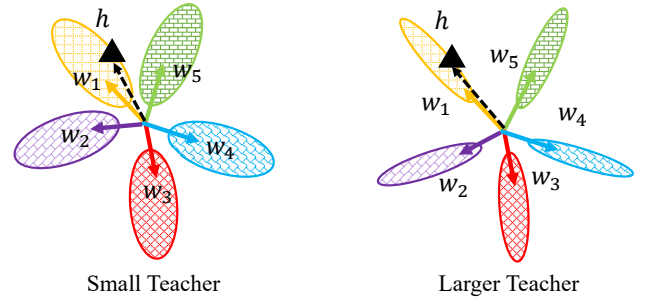


Fig. 4. Illustration of the classification layer with different feature compactness. The larger teacher may give a larger ground-truth logit or less varied non-ground-truth logits.

This will lead to a larger logit for the ground-truth class. If the intra-class features are nearly orthogonal, the logits for non-ground-truth classes will be less varied. The illustration can be found in Fig. 4, where the larger teacher extracts more compact inter-class features and more dispersed intra-class features. The triangle represents a sample feature in the 1-st class, and the larger teacher tends to give a larger target logit (i.e., $\mathbf{f}_1 = \mathbf{h}^T \mathbf{w}_1$) and less varied non-ground-truth class logits (i.e., $\mathbf{g} = [\mathbf{h}^T \mathbf{w}_c]_{c \in \{2,3,4,5\}}$). A larger target logit or less varied non-ground-truth class logits will both lead to less varied non-ground-truth class probabilities after applying softmax function [31]. The step-by-step analysis and visualization provide explanations for the first observation that larger teachers tend to produce probability vectors that are less varied between non-ground-truth classes.

C. The Relative Class Affinities

The second observation in Sect. IV-A implies that the relative probability values given by different teachers seem to be consistent. Hence, we explore this observation further through several quantitative metrics. The intuitive idea is to explore whether different teachers give the same top- K predictions or not. Specifically, we train a smaller teacher t_{small} and a larger teacher t_{large} on the same dataset. Then, we calculate the predicted top- K classes for the i -th training sample, and denote the predicted class sets as $\mathcal{C}_{i,K}^{\text{large}}$ and $\mathcal{C}_{i,K}^{\text{small}}$, respectively. We denote $|\mathcal{C}_{i,K}^{\text{large}} \cap \mathcal{C}_{i,K}^{\text{small}}|$ as the number of overlapped classes. Then we show the distribution of the number of overlapped classes when considering different K . Fig. 5 displays the results on CUB and TinyImageNet. The percentages in the figure show how many data samples have the number of overlapping classes corresponding to the values of the y-axis. Considering the top-3 predicted classes of ResNeXt50-32-4d and ResNeXt101-32-8d on CUB, there are 21.6% training samples that have 3 common predicted classes, and 56.4% training samples that have 2 common predicted classes. If we consider top-8 predicted classes, there are nearly 69.4% training samples that have at least 5 common predicted classes. This implies that different teachers indeed have a great deal of consistency in top- K class recognition.

Then, we define several specific metrics to further explore the consistency. The first metric is named the rank set overlap

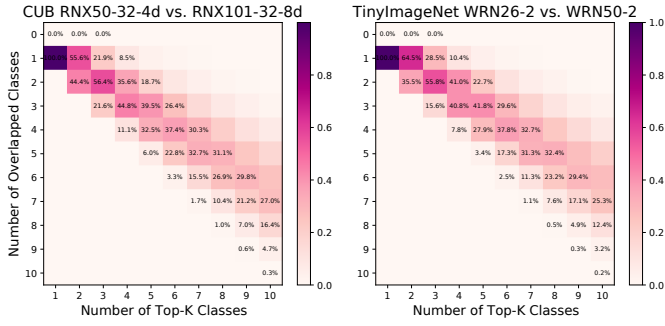


Fig. 5. The predicted top- K class set overlap of a smaller and a larger teacher network on two datasets. The x-axis shows K and the y-axis shows the number of overlapped classes.

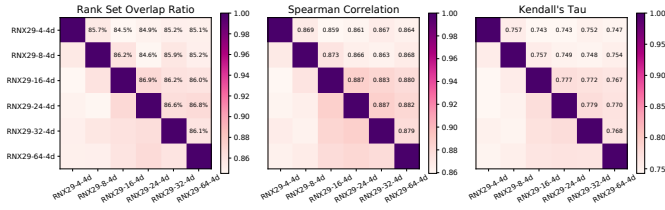


Fig. 6. Several magnitude-agnostic metrics that measure the consistency of relative class affinities between teacher networks with various capacities. The used dataset is CIFAR-10.

ratio, which is calculated as follows:

$$s_i(t_1, t_2) = |\mathcal{C}_{i,K}^{t_1} \cap \mathcal{C}_{i,K}^{t_2}| / K, \quad (3)$$

where t_1, t_2 denote teachers. The second metric is the Spearman correlation. It first obtains the rank of all classes in the output logits of two teachers, i.e., $\mathbf{R}_i^t = \text{argsort}(\mathbf{f}_i^t)$, $t \in \{t_1, t_2\}$. Then, it calculates the Pearson correlation as follows:

$$\rho_i(t_1, t_2) = \frac{\sum_{j=1}^C (\mathbf{R}_{i,j}^{t_1} - \overline{\mathbf{R}_i^{t_1}}) (\mathbf{R}_{i,j}^{t_2} - \overline{\mathbf{R}_i^{t_2}})}{\sqrt{\sum_{j=1}^C (\mathbf{R}_{i,j}^{t_1} - \overline{\mathbf{R}_i^{t_1}})^2 \sum_{j=1}^C (\mathbf{R}_{i,j}^{t_2} - \overline{\mathbf{R}_i^{t_2}})^2}}, \quad (4)$$

where j is the index of class and $\overline{\mathbf{R}_i^t}$ means the average of the elements in \mathbf{R}_i^t . Finally, we calculate Kendall's τ between $\mathbf{f}_i^{t_1}$ and $\mathbf{f}_i^{t_2}$, which directly shows the rank correlation of two teachers. The formulation is:

$$\tau_i(t_1, t_2) = \frac{2}{C(C-1)} \sum_{j_1 < j_2} \text{sg}(\mathbf{f}_{i,j_1}^{t_1} - \mathbf{f}_{i,j_2}^{t_1}) \text{sg}(\mathbf{f}_{i,j_1}^{t_2} - \mathbf{f}_{i,j_2}^{t_2}), \quad (5)$$

where j_1 and j_2 show the index of classes. C is the number of classes, and $\text{sg}(\cdot)$ returns 1 or 0 depending on whether the input is positive or not. These three metrics only depend on classes' relative magnitudes and are irrelevant to the absolute values. The metrics are calculated on CIFAR-10 under a series of ResNeXt networks. We set $K = 5$ for the rank set overlap metric. The above equations only show the metrics on a single training sample, and we report the average result on 50K training samples. The results are in Fig. 6. Excitingly, these metrics among teachers with different capacities do not vary a lot, and the Spearman correlations are almost all larger than

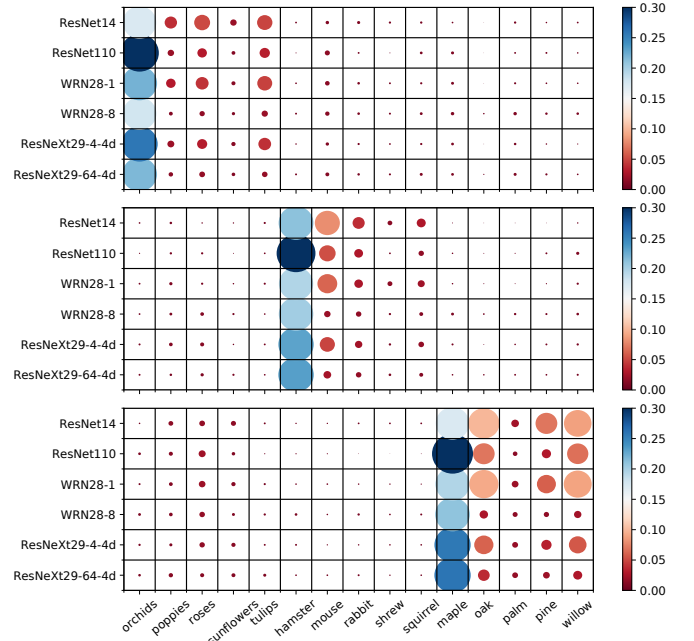


Fig. 7. The group classification on CIFAR-100. Each row shows the averaged posterior distribution given by a specific network. Circle size and color map determine the value. The three subfigures show results of fine-grained class “orchids”, “hamster”, and “maple”, respectively, which belong to the superclass “flowers”, “small mammals”, and “trees”. The x-axis shows the $3 \times 5 = 15$ fine-grained classes in the three superclasses.

0.85. According to the interpretation of Kendall's τ [68], [69], if the smaller teacher predicts that class j_1 is more related to the target class than that of class j_2 , then the larger teacher has a probability of 0.875 to give the same relative affinity. These metrics demonstrate that teachers know approximately the same about relative class affinities. Certainly, the output logits of different networks are not completely identical in order, even for the same networks under different training randomness [70], [71].

D. Verification by Group Classification

The probability vector \mathbf{p}^t inherently represents the posterior probability distribution predicted by a teacher network. During the training process, the cross-entropy loss minimizes the divergence between the posterior label distribution and the empirical “one-hot” label distribution. The “one-hot” labels cannot introduce class relations into the learning process. Hence, the teacher's label could be viewed as an alternate that could help the student grasp the affinities between classes. However, we do not know the real posterior distribution of each training sample and cannot judge which teacher's label is better.

Although it is hard to assign the real posterior distribution for each training sample, the group classification scenes could provide some prior information between categories. CIFAR-100 contains 100 categories, which contain 20 superclasses and 5 classes for each superclass¹. For example, the superclass “flowers” contains five fine-grained classes includ-

¹<https://www.cs.toronto.edu/~kriz/cifar.html>

ing “orchids”, “poppies”, “roses”, “sunflowers” and “tulips”. One hypothesis is that categories in the same superclass are more similar to each other. We train different teachers on CIFAR-100 and find that the hypothesis holds true for most superclasses. Fig. 7 shows the averaged posterior distribution on three superclasses, i.e., “flowers”, “small mammals”, and “trees”. For each superclass, we select its first fine-grained class as the target label, i.e., “orchids”, “hamster”, and “maple”. For each target label, we obtain its corresponding training samples, i.e., 500 samples for each. We calculate the averaged probabilities via $\mathbb{E}_{\mathbf{x}, y=c}[\mathbf{p}^t(\mathbf{x}; \tau)]$ for c being one of the three target classes. We set τ as 4.0. The teacher network ranges from ResNet14 to ResNeXt29-64-4d. The circle size and color map represent the probability value. Obviously, for a specific fine-grained class, the predicted probability values for the classes in the same group are larger than other classes. Additionally, the relative probability values for the classes in the same group are basically consistent among the investigated networks. For example, different teacher networks agree that fine-grained classes “oak” and “willow” are more relevant to the target category “maple”, while “palm” is less relevant. Although teachers are consistent in the relative class affinities, the variance of the probability values becomes smaller as the teacher capacity increases. For example, the difference in circle sizes in the last row is much smaller than that in the first row, which behaves similarly in each subfigure.

Then we provide some rules that define the similarity between classes. For example, the rule “ $c_1: c_2, c_3, c_4, c_5$ ” represents that a sample in class c_1 is predicted with the following rank: $\mathbf{p}_{c_1} > \mathbf{p}_{c_2} > \mathbf{p}_{c_3} > \mathbf{p}_{c_4} > \mathbf{p}_{c_5}$. If a network gives the rank as “ c_1, c_3, c_2, c_4, c_5 ”, then the Kendall’s τ between the prediction and the rule is 0.8. To measure the absolute difference in the predictions of non-ground-truth classes, we also calculate the standard deviation of the probabilities, i.e., $\sigma([\mathbf{p}_{c_2}, \mathbf{p}_{c_3}, \mathbf{p}_{c_4}, \mathbf{p}_{c_5}])$. The following lists the rules defined in CIFAR-100:

- **C.1:** hamster: mouse, rabbit, squirrel, shrew
- **C.2:** orchids: tulips, roses, poppies, sunflowers
- **C.3:** maple: oak, willow, pine, palm
- **C.4:** dolphin: whale, seal, otter, mammals beaver
- **C.5:** apples: sweet peppers, oranges, pears, mushrooms

The above rules are concluded from the averaged posterior probability distributions shown in Fig. 7. Notably, we only consider the class relationship in the same superclass for simplification. Additionally, we also construct a group classification task that utilizes five digits classification datasets, i.e., MNIST, MNISTM, USPS, SVHN, SYN. We denote this as Digits-Five, which is often used in domain adaptation tasks [38] or task relationship estimation [72]. The construction process is simple where we only centralize the data together and obtain a task with $5 \times 10 = 50$ classes. According to the transfer performances and the task relation coefficients presented in the previous works [38], [72], we abstract several rules as follows:

- **D.1:** MNIST@ c : USPS@ c , SVHN@ c
- **D.2:** MNIST@ c : MNISTM@ c , SYN@ c
- **D.3:** USPS@ c : MNIST@ c , MNISTM@ c , SVHN@ c

TABLE I
THE CONSISTENCY BETWEEN THE RANKS PREDICTED BY DIFFERENT TEACHERS WITH THE DEFINED RULES AND THE STANDARD DEVIATION OF THE NON-GROUND-TRUTH CLASS PROBABILITY VALUES.

CIFAR-100	Kendall’s τ			Standard Deviation		
	ResNet20	WRN28-3	RNX29-64-4d	ResNet20	WRN28-3	RNX29-64-4d
C.1	0.811	0.845	0.842	0.023	0.010	0.007
C.2	0.596	0.513	0.430	0.017	0.005	0.004
C.3	0.436	0.444	0.525	0.036	0.015	0.010
C.4	0.776	0.824	0.849	0.026	0.012	0.010
C.5	0.593	0.658	0.587	0.024	0.009	0.007
Avg	0.643	0.657	0.647	0.025	0.010	0.008

Digits	Kendall’s τ			Standard Deviation		
	VGG8	VGG13	VGG19	VGG8	VGG13	VGG19
D.1	0.994	0.996	0.993	0.008	0.004	0.003
D.2	0.991	0.999	0.998	0.010	0.007	0.005
D.3	0.904	0.870	0.910	0.009	0.009	0.007
Avg	0.963	0.955	0.967	0.009	0.007	0.005

MNIST@ c represents the c -th class in MNIST, and others are defined similarly. Each of the above rules contains a group of fine-grained rules if we set $c \in \{0, 1, \dots, 9\}$. Hence, the averaged results across the fine-grained ones are reported for each rule.

Although it is difficult to claim that the above rules apply to all samples of the corresponding class, the rules may provide a potentially approximate estimation for the real posterior of a specific sample. Tab. I lists the results of Kendall’s τ and the standard deviation of non-ground-truth classes’ probabilities. The consistency degrees of teachers’ outputs with the defined rules do not vary obviously. The predicted ranks are almost completely consistent in the simpler classification task, i.e., Kendall’s τ is almost near 1.0 in Digits Five. However, the standard deviations of larger teachers are much smaller than those of smaller teachers, implying that larger teachers’ outputs are less varied between non-ground-truth classes. These experimental studies on group classification verify the initial observations in Sect. IV-A again.

V. ADDRESSING CAPACITY MISMATCH

As introduced in Sect. III, the “capacity mismatch” refers to the phenomenon that larger networks may not teach students as well as smaller teachers [31]–[33], [35], [36]. The above observations show that the relative class affinity between the larger teacher and smaller teacher’s outputs are basically consistent, while the absolute probabilities between non-ground-truth classes are not so discriminative for larger teachers. Hence, our proposed methods aim to enhance the distinctness between non-ground-truth class probabilities from different perspectives.

A. Fusing Global Class Relations (FGCR)

For each class c , we calculate the averaged probabilities via $\mathbb{E}_{\mathbf{x}, y=c}[\mathbf{p}(\mathbf{x}; \tau_0)]$, and advocate that this captures the global relationships among classes. According to Fig. 7, the global relationships given by different teachers are similar in relative

values, which may be useful for stable distillation. Hence, we fuse this to each training sample of the c -th class as follows:

$$\hat{\mathbf{p}}(\mathbf{x}; \tau) = (1.0 - \alpha)\mathbf{p}(\mathbf{x}; \tau) + \alpha * \mathbb{E}_{\mathbf{x}, y=c}[\mathbf{p}(\mathbf{x}; \tau_0)], \quad (6)$$

where α is the hyper-parameter. We empirically found that setting $\tau_0 < \tau$ for calculating the averaged probabilities could enhance the variance of non-ground-truth class probabilities. As shown in Fig. 7, the averaged probability distribution provided by larger networks still shows less varied values among non-ground-truth classes, which may limit the effectiveness of this method. Hence, we only provide this method as a trial, and it is not the focus of our paper. In fact, the performances of FGCR could surpass the distillation performance of a smaller teacher, while it is still worse than other advanced techniques as shown in Tab. II.

B. Regularizing Teachers (RegT)

. During the phase of training teachers, we add the following regularization to enhance the variance of non-ground-truth class probabilities:

$$\ell(\mathbf{x}, y) = \ell_{\text{CE}}(\mathbf{x}, y) + \beta (\mathbf{p}_y(\mathbf{x}; 1.0) - \sigma(\mathbf{q}(\mathbf{x}; 1.0))), \quad (7)$$

where $\mathbf{q}(\mathbf{x}; 1.0) = [\mathbf{p}_c(\mathbf{x}; 1.0)]_{c \neq y}$ and β is the coefficient of the regularization term. The loss function explicitly encourages the teacher network to decrease the influence of the ground-truth class and enhance the distinctness of non-ground-truth classes. Different from other post-processing methods, this way could enhance the variance of non-ground-truth class probabilities in the stage of training teachers.

C. Instance-Specific Asymmetric Temperature Scaling (ISATS)

. The previous work [31] proposes the approach named asymmetric temperature scaling (ATS) to tackle the capacity mismatch in KD. ATS applies different temperatures to the logits of ground-truth and non-ground-truth classes, i.e.,

$$\mathbf{p}_c(\tau_1, \tau_2) = \exp(\mathbf{f}_c/\tau_c) / \sum_{j \in [C]} \exp(\mathbf{f}_j/\tau_j), \quad (8)$$

where $\tau_j = \tau_1$ for $j = y$ and $\tau_j = \tau_2$ for $j \neq y$. The recommended setting is $\tau_1 - \tau_2 \in [1, 2]$. This could effectively make the larger networks teach well again, but the effort in searching for proper hyper-parameters of τ_1 and τ_2 is huge.

As a step further solution, we extend ATS to Instance-Specific ATS (ISATS) that searches for proper temperatures for each training sample. Given a training sample \mathbf{x} , the predicted logit vector is $\mathbf{f}(\mathbf{x})$, and the optimal temperature that could enlarge the variance of softened non-ground-truth classes' probabilities is:

$$\tau^*(\mathbf{x}) = \arg \max_{\tau} v(\mathbf{q}(\mathbf{x}; \tau)), \quad (9)$$

where $\mathbf{q}(\mathbf{x}; \tau)$ denotes the probability vector of non-ground-truth classes, i.e., $\mathbf{q}(\mathbf{x}; \tau) = [\mathbf{p}_c(\mathbf{x}; \tau)]_{c \neq y}$ and $\mathbf{p}(\mathbf{x}; \tau) = \text{SF}(\mathbf{f}(\mathbf{x}); \tau)$. $v(\cdot)$ calculates the variance of the elements in a vector. That is, the optimal temperature for each instance is searched to make the probabilities of non-ground-truth classes more distinct. Then, we set $\tau_1(\mathbf{x}) = \tau^* + 1$ and $\tau_2(\mathbf{x}) = \tau^*$ as

recommended by ATS [31]. Compared with ATS, the proposed ISATS has two advantages. First, ISATS saves the effort of finding the proper value of τ_2 , and thus the setting of τ_1 could also be quickly determined. Second, ISATS considers a more fine-grained way to release the discriminative information contained in non-ground-truth classes for each training sample. Therefore, ISATS could commonly obtain better performances than ATS.

VI. PERFORMANCE COMPARISONS

This section provides performance comparisons of addressing capacity mismatch in KD. The experimental studies follow the settings in [31] and utilize the publicly available code ². We directly cite some experimental results for comparisons. Specifically, the utilized datasets are CIFAR-10/CIFAR-100 [37], TinyImageNet [59], CUB [57], and Stanford Dogs [56]. Teacher networks include versions of ResNet [54], WideResNet [58], and ResNeXt [55]. Student networks are VGG [61], ShuffleNetV1/V2 [4], [5], AlexNet [73], and MobileNetV2 [3]. We train networks on corresponding datasets for 240 epochs. SGD optimizer with a momentum value of 0.9 is used. The learning rate is 0.05 by default, and the batch size is 128. For our proposed FGCR, we set $\tau_0 = \tau - 1$ and $\alpha \in \{0.1, 0.5\}$, and the best results are reported. For RegT, β is searched in $\{0.01, 0.001\}$. For ISATS, we search for the best temperature for each instance in the scope of $\{1.0, 2.0, 3.0, 4.0, 5.0, 6.0, 8.0\}$. The distribution of the optimal instance-specific temperatures on CIFAR-100 is as follows: 4.0 accounts for about 31%, 5.0 accounts for about 27%, 3.0 accounts for about 22%, and others account for 20%.

A. Performance Comparisons

We compare with SOTA methods and list the results on CIFAR-100, TinyImageNet, CUB, and Dogs in Tab. II. The compared methods include ESKD [32], TAKD [33], SCKD [34], and ATS [31]. NoKD trains students without the teacher's supervision. ST-KD trains students under the guidance of a smaller teacher. KD trains students under the guidance of the larger teacher. The larger teachers are ResNet110, WRN50-2, RNx101-32-8d, and RNx101-32-8d for the four datasets, while the smaller teachers are ResNet20, WRN26-2, RNx50-32-4d, and RNx50-32-4d, respectively. The values in “()” display the test accuracy of the large teachers. The last column of the table shows the average performance of corresponding rows. The last three rows present the performances of our proposed algorithms. These methods could improve the performances of students when taught by a larger network and surpass that of KD and ST-KD, which verifies that enhancing the variance of non-ground-truth classes could indeed make larger networks teach well again. The proposed ISATS could achieve the SOTA results when compared with ATS. It is easy to understand that ISATS searches for optimal temperatures in an instance-specific manner, which could enhance the variance of non-ground-truth class probabilities more effectively. RegT belongs

²<https://github.com/lxcnju/ATS-LargeKD>

TABLE II
PERFORMANCE COMPARISONS OF ADDRESSING CAPACITY MISMATCH IN KD. THE LAST THREE ROWS ARE OUR METHODS.

Dataset	CIFAR-100			TinyImageNet			CUB			Stanford Dogs			Avg
Teacher	ResNet110 (74.09)			WRN50-2(66.28)			RNx101-32-8d (79.50)			RNx101-32-8d (73.98)			
Student	VGG8	SFV1	MV2	ANet	SFV2	MV2	ANet	SFV2	MV2	ANet	SFV2	MV2	
NoKD	69.92	70.04	64.75	34.62	45.79	52.03	55.66	71.24	74.49	50.20	68.72	68.67	60.51
ST-KD	72.30	73.22	66.56	36.16	49.59	52.93	56.39	72.15	76.80	51.95	69.92	72.06	62.50
KD	71.35	71.86	65.49	35.83	48.48	52.33	55.10	71.89	76.45	50.22	68.48	71.25	61.56
ESKD	71.88	72.02	65.92	34.97	48.34	52.15	55.64	72.15	76.87	50.39	69.02	71.56	61.74
TAKD	72.71	72.86	66.98	36.20	48.71	52.44	54.82	71.53	76.25	50.36	68.94	70.61	61.87
SCKD	70.38	70.61	64.59	36.16	48.76	51.83	56.78	71.99	75.13	51.78	68.80	70.13	61.41
DIST	71.22	71.10	65.01	35.95	45.75	50.56	48.88	71.79	75.34	49.85	67.69	68.97	60.18
KD+ATS	72.31	73.44	67.18	37.42	50.03	54.11	58.32	73.15	77.83	52.96	70.92	73.16	63.40
KD+FGCR	71.99	72.42	66.39	35.70	48.35	53.25	60.22	73.63	79.44	51.84	70.45	72.98	63.05
KD+RegT	72.09	72.39	66.18	36.66	48.48	53.31	60.17	74.20	79.21	52.18	70.55	72.43	63.15
KD+ISATS	72.46	73.80	67.04	37.15	49.61	55.49	61.73	74.23	78.84	54.36	70.98	72.73	64.04

TABLE III
ENSEMBLE PERFORMANCE COMPARISONS OF ADDRESSING CAPACITY MISMATCH IN KD. THE LAST THREE ROWS ARE OUR METHODS.

Dataset	CIFAR-100			TinyImageNet			CUB			Stanford Dogs			Avg
Teacher	ResNet110 (74.09)			WRN50-2(66.28)			RNx101-32-8d (79.50)			RNx101-32-8d (73.98)			
Student	VGG8	SFV1	MV2	ANet	SFV2	MV2	ANet	SFV2	MV2	ANet	SFV2	MV2	
NoKD Ens	72.77	73.61	67.76	39.37	50.69	56.40	59.84	74.43	77.47	54.04	71.65	72.53	64.21
ResKD	73.89	76.03	69.00	38.66	51.93	57.32	62.60	75.29	76.27	54.68	70.73	72.85	64.94
KD+ATS+Ens	74.86	75.05	69.50	40.42	52.14	58.47	62.00	76.26	78.97	55.69	73.22	74.67	65.94
KD+FGCR+Ens	73.69	74.76	68.22	39.20	52.71	56.44	61.94	76.84	80.37	54.25	72.70	74.83	65.50
KD+RegT+Ens	74.88	74.95	68.45	39.37	53.78	57.35	62.11	75.64	80.82	55.03	72.73	74.25	65.78
KD+ISATS+Ens	74.55	74.43	68.61	40.25	53.18	58.78	63.82	75.07	80.87	56.62	73.53	75.30	66.25

to the pre-processing method that enhances the variance of non-ground-truth classes during the phase of training teachers, which also presents good performances.

We also verify the ensemble performances after distillation because ResKD [35], [36] improves the students' performances by introducing the residual student and taking the two residual students' ensemble. Although ResKD surpasses the performance of ATS, this comparison is not fair. Hence, we also provide ensemble performances of two separately trained students under different initialization and training seeds. For a fair comparison, we also test the performances of our methods by repeating the corresponding algorithms two times and making predictions via the ensemble of the obtained two student networks. The results are listed in Tab. III. Clearly, our proposed ISATS could also achieve better performances when compared with ATS and other methods.

B. Comparing ISATS with TS and ATS

We then especially focus on the comparison of ISATS with TS and ATS. Specifically, we follow the experimental settings in [31] and additionally plot the performance curves when utilizing our proposed ISATS. Fig. 8 shows several pairs of KD experimental studies, which include the combinations of three series of teacher networks (i.e., ResNet, WideResNet, and ResNeXt) and three student networks (i.e., VGG8, ShuffleNetV1, and MobileNetV2). The utilized dataset is CIFAR-

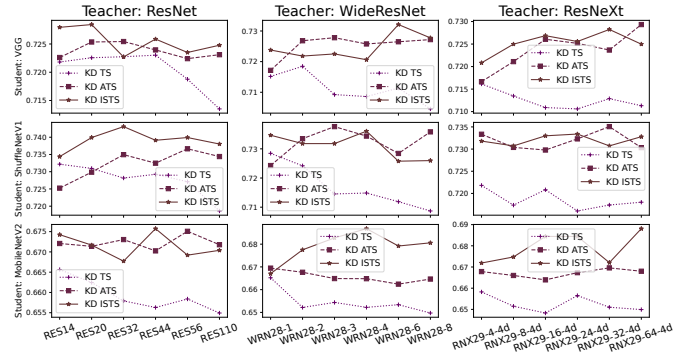


Fig. 8. Distillation results via TS, ATS, and ISATS on CIFAR-100. The x-axis of each figure shows teachers with various capacities.

100. Each plot shows three curves, including TS (i.e., KD), ATS (i.e., KD+TS), and ISATS (i.e., KD+ATS). The x-axis represents the increasing capacity of teachers. The curves of TS imply that the student's performance taught by teacher networks becomes worse when the teacher capacity increases, i.e., the capacity mismatch phenomenon. ATS could mitigate this phenomenon and make larger teachers teach well or better again. Our proposed ISATS has the same effect and could surpass ATS in most cases.

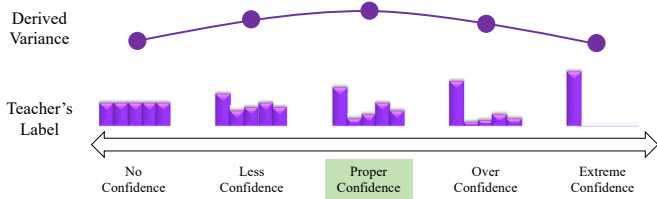


Fig. 9. The teacher’s label under different levels of confidence. The dark knowledge provided by the teacher with proper confidence is preferred.

VII. DISCUSSION

This paper explores the influence of teachers’ capacity on their provided distillation labels, i.e., the dark knowledge in KD. A larger teacher may be over-confident and provide probability vectors that are less discriminative between non-ground-truth classes. If we view the capacity as an influencing factor of the confidence level, then we could abstract the illustration shown in Fig. 9. In fact, the confidence level is related to the following factors.

- **Network Capacity.** This paper mainly explores this factor. An extremely smaller network tends to provide uniform predictions, while an extremely larger network provides “one-hot” ones.
- **Training Process.** With the training process of a network, it becomes more and more confident. In the beginning, it is ignorant and provides uniform predictions. After enough training steps, it may output “one-hot” vectors.
- **Temperature Factor.** Given a trained network, we could also adjust the temperature and obtain different types of probability vectors. If we take a very high temperature, the distribution becomes uniform. In contrast, a lower temperature leads to “one-hot” results.

As shown in Fig. 9, a proper confidence level could generate a rational probability distribution that facilitates the KD process. For example, traditional KD methods do not use a too-small or too-large temperature [9]. Some works also point out that intermediate model checkpoints could be better teachers than the fully converged model [51]. That is, a proper training level of teachers also matters a lot in the KD process. Our work points out that the teacher with high capacity does not perform well in KD and proposes several solutions to adjust their over-confident outputs.

VIII. CONCLUSION

This paper studies the dark knowledge in KD under various teacher capacities. Two observations are first presented, i.e., the probability vectors provided by larger teachers are less distinct between non-ground-truth classes, while the relative probability values seem consistent between different teachers. Abundant experimental studies are provided to explain these two observations. The less varied non-ground-truth class probabilities make the student hardly grasp the absolute affinities of non-ground-truth classes to the target class, leading to the interesting “capacity mismatch” phenomenon in KD. Multiple effective and simple solutions are proposed to solve this problem. Finally, a unified perspective about dark knowledge under various confidence levels is provided for future studies.

REFERENCES

- [1] C. Bucila, R. Caruana, and A. Niculescu-Mizil, “Model compression,” in *Proceedings of the Twelfth ACM SIGKDD International Conference on Knowledge Discovery and Data Mining*, 2006, pp. 535–541.
- [2] A. G. Howard, M. Zhu, B. Chen, D. Kalenichenko, W. Wang, T. Weyand, M. Andreetto, and H. Adam, “Mobilenets: Efficient convolutional neural networks for mobile vision applications,” *CoRR*, vol. abs/1704.04861, 2017.
- [3] M. Sandler, A. G. Howard, M. Zhu, A. Zhmoginov, and L. Chen, “Mobilenetv2: Inverted residuals and linear bottlenecks,” in *2018 IEEE Conference on Computer Vision and Pattern Recognition*, 2018, pp. 4510–4520.
- [4] X. Zhang, X. Zhou, M. Lin, and J. Sun, “Shufflenet: An extremely efficient convolutional neural network for mobile devices,” in *2018 IEEE Conference on Computer Vision and Pattern Recognition*, 2018, pp. 6848–6856.
- [5] N. Ma, X. Zhang, H. Zheng, and J. Sun, “Shufflenet V2: practical guidelines for efficient CNN architecture design,” in *Computer Vision - ECCV 2018 - 15th European Conference*, 2018, pp. 122–138.
- [6] Z. Zhou, Y. Jiang, and S. Chen, “Extracting symbolic rules from trained neural network ensembles,” *AI Communications*, vol. 16, no. 1, pp. 3–15, 2003.
- [7] Z. Zhou and Y. Jiang, “Nec4.5: Neural ensemble based C4.5,” *IEEE Transactions on Knowledge and Data Engineering*, vol. 16, no. 6, pp. 770–773, 2004.
- [8] G. Urban, K. J. Geras, S. E. Kahou, Ö. Aslan, S. Wang, A. Mohamed, M. Philipose, M. Richardson, and R. Caruana, “Do deep convolutional nets really need to be deep and convolutional?” in *The 5th International Conference on Learning Representations*, 2017.
- [9] G. E. Hinton, O. Vinyals, and J. Dean, “Distilling the knowledge in a neural network,” *CoRR*, vol. abs/1503.02531, 2015.
- [10] J. Gou, L. Sun, B. Yu, L. Du, K. Ramamohanarao, and D. Tao, “Collaborative knowledge distillation via multiknowledge transfer,” *IEEE Transactions on Neural Networks and Learning Systems*, vol. 35, no. 5, pp. 6718–6730, 2024.
- [11] D. Lopez-Paz, L. Bottou, B. Schölkopf, and V. Vapnik, “Unifying distillation and privileged information,” in *The 4th International Conference on Learning Representations*, 2016.
- [12] M. Phuong and C. Lampert, “Towards understanding knowledge distillation,” in *Proceedings of the 36th International Conference on Machine Learning*, 2019, pp. 5142–5151.
- [13] A. K. Menon, A. S. Rawat, S. J. Reddi, S. Kim, and S. Kumar, “A statistical perspective on distillation,” in *Proceedings of the 38th International Conference on Machine Learning*, 2021, pp. 7632–7642.
- [14] J. Gou, B. Yu, S. J. Maybank, and D. Tao, “Knowledge distillation: A survey,” *International Journal of Computer Vision*, vol. 129, no. 6, pp. 1789–1819, 2021.
- [15] A. Romero, N. Ballas, S. E. Kahou, A. Chassang, C. Gatta, and Y. Bengio, “Fitnets: Hints for thin deep nets,” in *The 3rd International Conference on Learning Representations*, 2015.
- [16] S. Zagoruyko and N. Komodakis, “Paying more attention to attention: Improving the performance of convolutional neural networks via attention transfer,” in *The 5th International Conference on Learning Representations*, 2017.
- [17] Z. Huang and N. Wang, “Like what you like: Knowledge distill via neuron selectivity transfer,” *CoRR*, vol. abs/1707.01219, 2017.
- [18] B. Heo, M. Lee, S. Yun, and J. Y. Choi, “Knowledge transfer via distillation of activation boundaries formed by hidden neurons,” in *The Thirty-Third AAAI Conference on Artificial Intelligence*, 2019, pp. 3779–3787.
- [19] N. Passalis and A. Tefas, “Learning deep representations with probabilistic knowledge transfer,” in *Computer Vision - ECCV 2018 - 15th European Conference*, vol. 11215, 2018, pp. 283–299.
- [20] C. K. Joshi, F. Liu, X. Xun, J. Lin, and C. S. Foo, “On representation knowledge distillation for graph neural networks,” *IEEE Transactions on Neural Networks and Learning Systems*, vol. 35, no. 4, pp. 4656–4667, 2024.
- [21] B. Peng, X. Jin, D. Li, S. Zhou, Y. Wu, J. Liu, Z. Zhang, and Y. Liu, “Correlation congruence for knowledge distillation,” in *2019 IEEE/CVF International Conference on Computer Vision*, 2019, pp. 5006–5015.
- [22] Y. Tian, D. Krishnan, and P. Isola, “Contrastive representation distillation,” in *The 8th International Conference on Learning Representations*, 2020.
- [23] J. Yim, D. Joo, J. Bae, and J. Kim, “A gift from knowledge distillation: Fast optimization, network minimization and transfer learning,” in 2017

- IEEE Conference on Computer Vision and Pattern Recognition*, 2017, pp. 7130–7138.
- [24] Y. Liu, J. Cao, B. Li, C. Yuan, W. Hu, Y. Li, and Y. Duan, “Knowledge distillation via instance relationship graph,” in *IEEE Conference on Computer Vision and Pattern Recognition*, 2019, pp. 7096–7104.
- [25] L. Yu, V. O. Yazici, X. Liu, J. van de Weijer, Y. Cheng, and A. Ramisa, “Learning metrics from teachers: Compact networks for image embedding,” in *IEEE Conference on Computer Vision and Pattern Recognition*, 2019, pp. 2907–2916.
- [26] F. Tung and G. Mori, “Similarity-preserving knowledge distillation,” in *2019 IEEE/CVF International Conference on Computer Vision*, 2019, pp. 1365–1374.
- [27] H. Ye, S. Lu, and D. Zhan, “Distilling cross-task knowledge via relationship matching,” in *2020 IEEE/CVF Conference on Computer Vision and Pattern Recognition*, 2020, pp. 12 393–12 402.
- [28] J. Liu, D. Wen, H. Gao, W. Tao, T. Chen, K. Osa, and M. Kato, “Knowledge representing: Efficient, sparse representation of prior knowledge for knowledge distillation,” in *IEEE Conference on Computer Vision and Pattern Recognition Workshops*, 2019, pp. 638–646.
- [29] X. Li, Y. Grandvalet, and F. Davoine, “Explicit inductive bias for transfer learning with convolutional networks,” in *Proceedings of the 35th International Conference on Machine Learning*, 2018, pp. 2830–2839.
- [30] S. Li, M. Lin, Y. Wang, Y. Wu, Y. Tian, L. Shao, and R. Ji, “Distilling a powerful student model via online knowledge distillation,” *IEEE Transactions on Neural Networks and Learning Systems*, vol. 34, no. 11, pp. 8743–8752, 2023.
- [31] X. Li, W. Fan, S. Song, Y. Li, B. Li, Y. Shao, and D. Zhan, “Asymmetric temperature scaling makes larger networks teach well again,” in *Advances in Neural Information Processing Systems 35*, 2022.
- [32] J. H. Cho and B. Hariharan, “On the efficacy of knowledge distillation,” in *IEEE/CVF International Conference on Computer Vision*, 2019, pp. 4793–4801.
- [33] S. Mirzadeh, M. Farajtabar, A. Li, N. Levine, A. Matsukawa, and H. Ghasemzadeh, “Improved knowledge distillation via teacher assistant,” in *The Thirty-Fourth AAAI Conference on Artificial Intelligence*, 2020, pp. 5191–5198.
- [34] Y. W. Yichen Zhu, “Student customized knowledge distillation: Bridging the gap between student and teacher,” in *IEEE/CVF International Conference on Computer Vision*, 2021.
- [35] M. Gao, Y. Wang, and L. Wan, “Residual error based knowledge distillation,” *Neurocomputing*, vol. 433, pp. 154–161, 2021.
- [36] X. Li, S. Li, B. Omar, F. Wu, and X. Li, “Reskd: Residual-guided knowledge distillation,” *IEEE Transactions on Image Processing*, vol. 30, pp. 4735–4746, 2021.
- [37] A. Krizhevsky, “Learning multiple layers of features from tiny images,” 2012.
- [38] Y. Ganin and V. S. Lempitsky, “Unsupervised domain adaptation by backpropagation,” in *Proceedings of the 32nd International Conference on Machine Learning*, 2015, pp. 1180–1189.
- [39] J. Tang, R. Shivanna, Z. Zhao, D. Lin, A. Singh, E. H. Chi, and S. Jain, “Understanding and improving knowledge distillation,” *CoRR*, vol. abs/2002.03532, 2020.
- [40] G. Ji and Z. Zhu, “Knowledge distillation in wide neural networks: Risk bound, data efficiency and imperfect teacher,” in *Advances in Neural Information Processing Systems 33*, 2020.
- [41] L. Yuan, F. E. H. Tay, G. Li, T. Wang, and J. Feng, “Revisiting knowledge distillation via label smoothing regularization,” in *2020 IEEE/CVF Conference on Computer Vision and Pattern Recognition*, 2020, pp. 3902–3910.
- [42] T. Dao, G. M. Kamath, V. Syrgkanis, and L. Mackey, “Knowledge distillation as semiparametric inference,” in *The 9th International Conference on Learning Representations*, 2021.
- [43] H. Zhou, L. Song, J. Chen, Y. Zhou, G. Wang, J. Yuan, and Q. Zhang, “Rethinking soft labels for knowledge distillation: A bias-variance tradeoff perspective,” in *The 9th International Conference on Learning Representations*, 2021.
- [44] D. Hsu, Z. Ji, M. Telgarsky, and L. Wang, “Generalization bounds via distillation,” in *The 9th International Conference on Learning Representations*, 2021.
- [45] X. Cheng, Z. Rao, Y. Chen, and Q. Zhang, “Explaining knowledge distillation by quantifying the knowledge,” in *2020 IEEE/CVF Conference on Computer Vision and Pattern Recognition*, 2020, pp. 12 922–12 932.
- [46] R. Müller, S. Kornblith, and G. E. Hinton, “When does label smoothing help?” in *Advances in Neural Information Processing Systems 32*, 2019, pp. 4696–4705.
- [47] Z. Shen, Z. Liu, D. Xu, Z. Chen, K. Cheng, and M. Savvides, “Is label smoothing truly incompatible with knowledge distillation: An empirical study,” in *The 9th International Conference on Learning Representations*, 2021.
- [48] T. Furlanello, Z. C. Lipton, M. Tschannen, L. Itti, and A. Anandkumar, “Born-again neural networks,” in *Proceedings of the 35th International Conference on Machine Learning*, vol. 80, 2018, pp. 1602–1611.
- [49] C. Tan and J. Liu, “Improving knowledge distillation with a customized teacher,” *IEEE Transactions on Neural Networks and Learning Systems*, vol. 35, no. 2, pp. 2290–2299, 2024.
- [50] T. Huang, S. You, F. Wang, C. Qian, and C. Xu, “Knowledge distillation from A stronger teacher,” in *Advances in Neural Information Processing Systems 35*, 2022.
- [51] C. Wang, Q. Yang, R. Huang, S. Song, and G. Huang, “Efficient knowledge distillation from model checkpoints,” in *Advances in Neural Information Processing Systems 35*, 2022.
- [52] H. Ye, L. Ming, D. Zhan, and W. Chao, “Few-shot learning with a strong teacher,” *IEEE Transactions on Pattern Analysis and Machine Intelligence*, vol. 46, no. 3, pp. 1425–1440, 2024.
- [53] Y. Wang, B. Qian, H. Liu, Y. Rui, and M. Wang, “Unpacking the gap box against data-free knowledge distillation,” *IEEE Transactions on Pattern Analysis and Machine Intelligence*, pp. 1–12, 2024.
- [54] K. He, X. Zhang, S. Ren, and J. Sun, “Deep residual learning for image recognition,” in *IEEE Conference on Computer Vision and Pattern Recognition*, 2016, pp. 770–778.
- [55] S. Xie, R. B. Girshick, P. Dollár, Z. Tu, and K. He, “Aggregated residual transformations for deep neural networks,” in *IEEE Conference on Computer Vision and Pattern Recognition*, 2017, pp. 5987–5995.
- [56] A. Khosla, N. Jayadevaprakash, B. Yao, and F. fei Li, “Novel dataset for fine-grained image categorization,” in *First Workshop on Fine-Grained Visual Categorization, CVPR (2011)*.
- [57] C. Wah, S. Branson, P. Welinder, P. Perona, and S. Belongie, “The Caltech-UCSD Birds-200-2011 Dataset,” no. CNS-TR-2011-001, 2011.
- [58] S. Zagoruyko and N. Komodakis, “Wide residual networks,” in *Proceedings of the British Machine Vision Conference*, 2016.
- [59] A. Tavaneai, “Embedded encoder-decoder in convolutional networks towards explainable AI,” *CoRR*, vol. abs/2007.06712, 2020.
- [60] Y. Lecun, L. Bottou, Y. Bengio, and P. Haffner, “Gradient-based learning applied to document recognition,” *Proceedings of the IEEE*, vol. 86, no. 11, pp. 2278–2324, 1998.
- [61] K. Simonyan and A. Zisserman, “Very deep convolutional networks for large-scale image recognition,” in *3rd International Conference on Learning Representations*, 2015.
- [62] Y. Netzer, T. Wang, A. Coates, A. Bissacco, B. Wu, and A. Ng, “Reading digits in natural images with unsupervised feature learning,” 2011.
- [63] V. Nair and G. E. Hinton, “Rectified linear units improve restricted boltzmann machines,” in *Proceedings of the 27th International Conference on Machine Learning*, 2010, pp. 807–814.
- [64] L. van der Maaten, “Barnes-hut-sne,” in *1st International Conference on Learning Representations*, 2013.
- [65] R. A. Fisher, “The use of multiple measurements in taxonomic problems,” *Annals of Human Genetics*, vol. 7, pp. 179–188, 1936.
- [66] J. Yang, D. Zhang, J.-y. Yang, and B. Niu, “Globally maximizing, locally minimizing: Unsupervised discriminant projection with applications to face and palm biometrics,” *IEEE Transactions on Pattern Analysis and Machine Intelligence*, vol. 29, no. 4, pp. 650–664, 2007.
- [67] X. Li and D. Zhan, “Fedrs: Federated learning with restricted softmax for label distribution non-iid data,” in *KDD*, 2021, pp. 995–1005.
- [68] R. Fagin, R. Kumar, and D. Sivakumar, “Comparing top k lists,” *SIAM Journal on Discrete Mathematics*, vol. 17, no. 1, pp. 134–160, 2003.
- [69] K. You, Y. Liu, J. Wang, and M. Long, “Logme: Practical assessment of pre-trained models for transfer learning,” in *Proceedings of the 38th International Conference on Machine Learning*, 2021, pp. 12 133–12 143.
- [70] Y. Li, J. Yosinski, J. Clune, H. Lipson, and J. E. Hopcroft, “Convergent learning: Do different neural networks learn the same representations?” in *4th International Conference on Learning Representations*, 2016.
- [71] Y. Ren, Q. Guo, Z. Jin, S. Ravfogel, M. Sachan, B. Schölkopf, and R. Cotterell, “All roads lead to rome? exploring the invariance of transformers’ representations,” *CoRR*, vol. abs/2305.14555, 2023.
- [72] C. Shui, M. Abbasi, L. Robitaille, B. Wang, and C. Gagné, “A principled approach for learning task similarity in multitask learning,” in *Proceedings of the Twenty-Eighth International Joint Conference on Artificial Intelligence*, 2019, pp. 3446–3452.
- [73] A. Krizhevsky, I. Sutskever, and G. E. Hinton, “Imagenet classification with deep convolutional neural networks,” in *Advances in Neural Information Processing Systems 25*, 2012, pp. 1106–1114.